Enhancement in the perfection of orthorhombic lysozyme crystals grown in a high magnetic field (10 T)

Takao Sato,[a] Yusuke Yamada,[a] Shinya Saijo,[a] Tetsuya Hori,[a] Raita Hirose,[a] Nobuo Tanaka,[a] Gen Sazaki,[b,c] Kazuo Nakajima,[b] Noriyuki Igarashi,[d] Masahiko Tanaka[d] and Yoshiki Matsuura[e]*

[a]Department of Life Science, Graduate School of Bioscience and Biotechnology, Tokyo Institute of Technology, 4259 Nagatsuta, Midori-ku, Yokohama 226-8501, Japan, [b]Institute for Materials Research, Tohoku University, 2-1-1 Katahira, Aoba-ku, Sendai 980-8577, Japan, [c]CREST, Japan Science and Technology Corporation, 2-1-6 Sengen, Tsukuba 305-0047, Japan, [d]Institute of Materials Structure Science, High Energy Accelerator Research Organization, 1-1 Oho, Tsukuba 305-0801, Japan, and [e]Institute for Protein Research, Osaka University, 3-2 Yamadaoka, Suita, Osaka 565-0871, Japan

Correspondence e-mail:
matsuura@protein.osaka-u.ac.jp

Orthorhombic crystals of hen egg-white (HEW) lysozyme were grown in a homogeneous and static magnetic field of 10 T. All crystals grown at 10 T were oriented such that their crystallographic c axes were parallel to the magnetic field direction and showed a narrower average full-width at half-maximum (FWHM) of the rocking curve than those grown at 0 T. Rocking-width measurements were made at the BL-10A station at the Photon Factory, Tsukuba, Japan, using a high-resolution vertical-type four-circle diffractometer. Crystal perfection was evaluated using the FWHM of the rocking curve; the effects of the magnetic field on the quality of the crystals were examined by comparison of the FWHM of seven crystals grown at 10 and 0 T. The FWHMs of the reflections along the a, b and c axes decreased by 23.5, 35.3 and 27.8%, respectively, and those of other general reflections decreased by 17.4–42.2% in the crystals grown at high magnetic field. These results clearly showed that a magnetic field of 10 T improved the crystal perfection of the orthorhombic lysozyme crystals. As a result, the maximum resolution of X-ray diffraction increased from 1.3 Å at 0 T to 1.13 Å at 10 T. The magnetic field also affected the dimensions of the unit cell, increments being 0.2% for the a and c axes and 0.1% for the b axis, respectively. These facts suggest that the application of a high magnetic field during crystallization might result in remarkable enhancements in the diffraction power of protein crystals having magnetic anisotropy.

1. Introduction

There have been a number of recent reports concerning the effect of magnetic fields on protein crystallization. Effects on the orientation (Rothgeb & Oldfield, 1981; Sazaki *et al.*, 1997; Ataka *et al.*, 1997; Wakayama, 1998; Astier *et al.*, 1998; Yanagiya *et al.*, 1999; Sakurazawa *et al.*, 1999), the crystal habit (Sazaki *et al.*, 1997), the number (Sazaki *et al.*, 1997: Wakayama *et al.*, 1997) and the growth rate (Yanagiya *et al.*, 2000) of protein crystals have so far been reported. A homogeneous magnetic field has been observed to dampen natural convection, even in an aqueous electrolyte solution (Sazaki *et al.*, 1999), and decreased the number and growth rate of protein crystals. Thus, a magnetic field might be a useful experimental parameter to improve the quality of protein crystals by reducing natural convection, in this way acting similarly to microgravity. The effects of a magnetic torque on the orientation of magnetically anisotropic substances may also contribute to producing a crystal of decreased mosaic spread. To test this, we compared the diffraction qualities of orthorhombic lysozyme crystals grown at 0 and 10 T.

An enhancement of lysozyme protein crystal perfection has been observed on crystallization in microgravity by Snell *et al.* (1995), who reported an average mosaicity of the order of 0.005°. To evaluate a rocking width of this order, especially at the resolution limit, the use of highly collimated synchrotron radiation is indispensable (Fourme *et al.*, 1999). Our measurements were therefore performed at the Photon Factory (PF), Tsukuba, Japan. Here, we report the comparison of rocking widths of crystals grown at 0 and 10 T. The intensity data collection showed that the maximum resolution limit extended from 1.33 to 1.13 Å on applying a magnetic field of 10 T (Sato *et al.*, 1999). Comparison of the crystal structures will be described elsewhere.

2. Experimental

2.1. Crystallization in a magnetic field of 10 T

Sixfold recrystallized hen egg-white lysozyme (Seikagaku Kogyo Co. Ltd) was used without further purification. All other chemicals were of reagent grade. Orthorhombic lysozyme crystals were prepared by a conventional batch technique. Lysozyme was

Table 1
Crystal data and data-collection statistics of 10 and 0 T crystals.

The programs *DENZO* and *SCALEPACK* (Otwinowski & Minor, 1997) were used to process the data at the Photon Factory. The interactive program *DPS/MOSFLM/CCP*4 (Rossman & van Beek, 1999) was used for processing the data from the R-AXIS IV image-plate detector. The oscillation angles were optimized so that the the ratio of the numbers of observed reflections between full and partial reflections becomes approximately 2:1 on one flame. $R_{merge} = \sum|I_i - \langle I \rangle|/\sum I_i$, where I_i is the measured intensity of an individual reflection and $\langle I \rangle$ is the mean intensity of symmetry-related measurements of this reflection. Unit-cell parameters are the mean of the measurements for seven crystals grown at both 0 and 10 T using an AFC5 four-circle diffractometer with Mo $K\alpha$ radiation from a sealed-tube source operated at 50 kV and 30 mA at 296 K.

Crystal data.

	10 T	0 T	Change (%)
Space group	$P2_12_12_1$	$P2_12_12_1$	
Unit-cell parameters (Å)			
a	56.54 (3)	56.44 (4)	+0.18
b	73.83 (6)	73.73 (7)	+0.14
c	30.50 (2)	30.43 (2)	+0.23

Data-collection statistics.

	10 T		0 T	
	PF BL18B	R-AXIS IV	PF BL18B	R-AXIS IV
Beam sizes (mm)	0.2 × 0.2	0.3 × 0.3	0.2 × 0.2	0.3 × 0.3
Crystal sizes (mm)	0.45 × 0.5 × 2	0.3 × 0.3 × 1.3	0.5 × 0.5 × 2	0.5 × 0.4 × 0.5
Program used	*DENZO/ SCALEPACK*	*DPS/MOSFLM/ CCP4*	*DENZO/ SCALEPACK*	*DPS/MOSFLM/ CCP4*
Camera distance (mm)	430	100	430	100
Wavelength used (Å)	1.000	1.5418	1.000	1.5418
Oscillation angle (°)	1.2	2	1.5	2
Exposure time (s)	64	600	80	600
Frames	73	50	48	50
Oscillation region	87.6	100.0	72.0	100.0
Resolution limit (Å)	50–1.13	50–1.7	50–1.3	50–2.0
Completeness (%)	71.9	99.5	62.4	93.6
R_{merge} (%)	2.6	5.4	2.9	10.2
Number of independent reflections	34449	14601	20095	8477

dissolved in 50 m*M* sodium acetate buffer pH 4.5 to a final lysozyme concentration of 500 mg ml^{-1}. Sodium chloride solution (50 mg ml^{-1}) was prepared in the same buffer. A supersaturated solution was prepared by mixing an equal volume of the lysozyme solution and the sodium chloride solution and was transferred into 20 glass tubes and two glass dishes, having respective capacities of 200 and 800 µl. To prevent
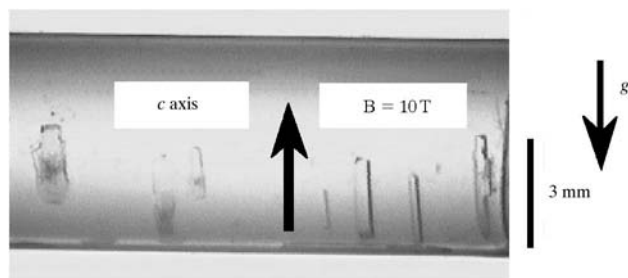

Figure 1
Orthorhombic lysozyme crystals grown in a magnetic field of 10 T. Almost all the crystals grew oriented such that their crystallographic *c* axes were parallel to the direction of the magnetic field. Crystallization conditions: 250 mg ml^{-1} lysozyme, 25 mg ml^{-1} NaCl in 50 m*M* sodium acetate buffer pH 4.5 at 313 K; 11 d duration. Dimensions of the orthorhombic lysozyme crystals used for data collection were typically 0.45 × 0.5 × 2.0 mm.

evaporation, the tubes were tightly capped and the dishes were covered by glass plates sealed with silicon grease.

Immediately after preparing the supersaturated solution, half the tubes and dishes were inserted into a temperature-controlled container (313.15 ± 0.1 K) and placed in the room-temperature bore of a liquid-helium-free superconducting magnet (JMTD-10T100M, Japan Magnet Technology Inc.). The bore was 100 mm in diameter and oriented vertically. The sample container was placed at the position of maximum field (the centre of the magnet). The homogeneity of the magnetic field within the sample container was better than 0.5%. Crystals were grown under a homogeneous and static magnetic field of 10 T for 11 d. The remaining tubes and dishes were placed in a

temperature-controlled incubator (313.15 ± 0.1 K) and used as a control experiment without a magnetic field. All of the crystallizations were set up within 10 min of mixing the solutions.

Fig. 1 shows a side view of the orthorhombic lysozyme crystals growing in a glass tube at 10 T. As shown in the figure, almost all of the crystals were oriented such that their crystallographic *c* axes were parallel to the direction of the magnetic field. Only the oriented crystals were used for X-ray experiments. At zero magnetic field, the crystals grew randomly oriented in the tubes and dishes. Although the data are not given here, the number of the crystals deposited at 10 T was much fewer than at zero magnetic field, as previously observed for tetragonal lysozyme and ferritin crystals (Sazaki *et al.*, 1997). In the absence of a magnetic field, the crystals appeared in nine out of ten tubes, compared with five out of ten at 10 T. These facts also suggest that magnetic damping of the natural convection in the tubes (Sazaki *et al.*, 1999) might play a role in decreasing secondary nucleation, *i.e.* the number of the nuclei subsequently produced by the flow of the solution in the vicinity of crystals or in contact with crystals in the post-nucleation phase.

2.2. X-ray analysis

The high magnetic field yielded relatively long crystals at 10 T compared with those at 0 T. A total of seven crystals for each case, *i.e.* high magnetic field and no magnetic field, were mounted in glass capillaries of 2.0 mm diameter for data collection. The approximate volume of the seven 10 T crystals ranged between 0.45 and 0.75 mm^3. An artificial mother liquor (2.2 *M* sodium chloride, 50 m*M* sodium acetate buffer pH 4.75) was used as a stabilizing solution. To prevent crystal slippage, a thin glass rod was inserted to attach the crystal. The approximate volume of the seven 0 T crystals ranged between 0.2 and 0.5 mm^3; they were mounted in the capillaries in the same way as the 10 T crystals.

Preliminary diffraction experiments were performed using a Rigaku AFC5 four-circle diffractometer and Mo $K\alpha$ radiation from a sealed tube with a focal size of 1 × 10 mm operated at 50 kV and 30 mA at 296 K. The unit-cell parameters and orientation matrices of seven different crystals grown at 0 and 10 T were determined using 20 reflections in the 2θ range 5–15°. The *a* and *c* unit-cell parameters increased by 0.2% and *b* by 0.1% (Table 1).

The crystals were then transferred to the four-circle diffractometer at BL10A at the PF. A rapid data-collection technique was employed for measurement of the rocking widths with monochromatic radiation. The instrument resolution function (IRF′) was calculated according to the method of Colapietro *et al.* (1992). The beamline supplies radiation of divergence 1.0 mrad from a bending magnet with a vertical beam size σ_y = 0.059 mm. A flat Si(111) crystal monochromator is located 12.5 m from the source, producing a beam of wavelength bandpass $\Delta\lambda/\lambda = 1.3 \times 10^{-4}$. Slit systems and a vertical-type four-circle diffractometer are located 2.5 m from the monochromator (Sasaki, 1989). The intensity-profile measurements were performed with a wavelength of 1.0 Å, where the Bragg angle of the monochromator was $\Theta = 9.431°$. The vertical beam divergence at the sample position was evaluated as Wd = 2.44×10^{-5} rad by the raytrace-simulation method (Muramatsu *et al.*, 1988); at the monochromator it was 2.16×10^{-5} rad and the source crossfire was 1.09×10^{-5} rad. The

dimension of the sample Cv = 0.5 mm and the source-to-instrument distance P = 15 m, yielding a crossfire contribution of (Cv/P) = 3.33×10^{-5} rad. Thus, we obtained IRF′ = 41 µrad = 0.0023°. The measurement was carried out for each crystal on the same index set of ten strong reflections (Table 2).

The rocking-curve profiles for some reflections are shown in Fig. 2. The full-width at half-maximum (FWHM) of each reflection was evaluated using the program *ORIGIN* (Press *et al.*, 1995) on a PC running Windows NT. The recorded intensity Y was calculated with peak fitting to a Gaussian distribution function of the form,

$$Y = Y_0 + \frac{A}{W(\pi/2)^{0.5}} \exp\left[\frac{2(X - X_0)^2}{W^2}\right],$$

where Y_0 is the baseline offset, A is the area size of the curve to the baseline, X_0 is the centre of a symmetric peak and W is twice the standard deviation, 2σ, and W is defined as approximately $0.849 \times$ FWHM. The FWHM of these curves ranges between 0.0051 and 0.0078° for 10 T, with an average

and σ of $0.0058 \pm 0.0012°$, and between 0.0059 and 0.0102° with an average and σ of $0.0081 \pm 0.0009°$ for 0 T, regardless of the size of the crystals. The reflection peak heights are based on the decrease only in mosaicity, as the 10 T crystals used were similar to or smaller than the 0 T crystals in size. The IRF′ of 0.0023° calculated above is essentially an insignificant contribution to the small value of 0.0051° including IRF′, as 0.0046° after IRF′ is deconvoluted out. These values are slightly larger than those of tetragonal crystals grown in microgravity (Snell *et al.*, 1995), which had reported FWHM values ranging from 0.0017 to 0.0100° with an average of 0.0047° for an IML2 shuttle mission microgravity-grown crystal, whereas the earth-grown control crystal had FWHM values ranging from 0.0067 to 0.0169° (an average of 0.0120°).

We then collected intensity data using a Weissenberg camera with an image plate on BL18B at PF. Of the 10 and 0 T crystals, those which showed good diffraction profiles were used for the intensity measurements. The crystals were mounted so that the X-ray
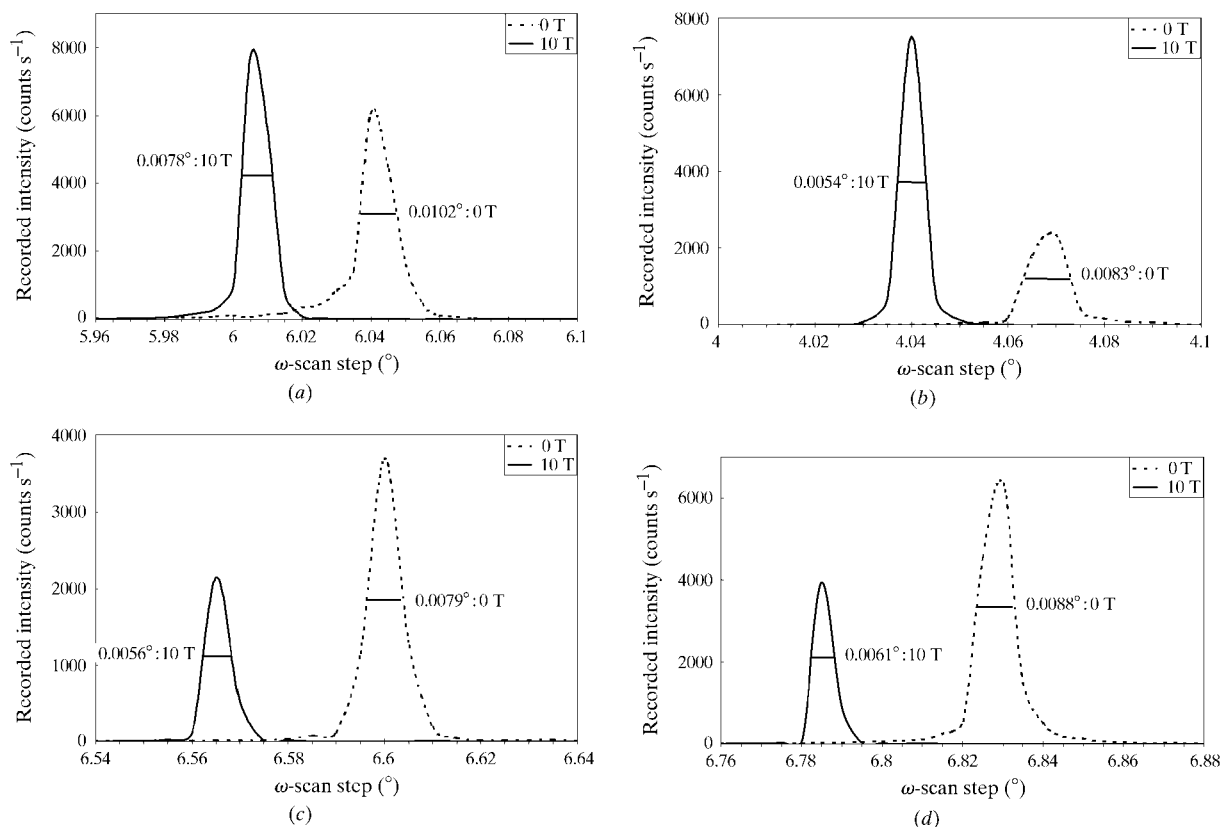

Figure 2
The ω-scan profiles of several reflections of 10 T crystals compared with 0 T crystals. Vertical axis, recorded intensity (counts s^{-1}); horizontal axis, ω angle with a step size of 0.005° (ideally a smaller step should have been used, but the curve fitting may mitigate for the use of the coarse step). Solid line, 10 T; dotted line, 0 T. The reflection peak heights of the comparison 10 T crystals are decreased compared with the crystals at 0 T, so that an attenuator was inserted so that the reflection intensity could not exceed 8000 counts s^{-1}. All curves were measured in single-bunch mode with an instrument resolution function of 0.0023°. The FWHM of the reflection has been evaluated in cases where the appreciable profile can be fitted to the main peak with a Gaussian distribution. These values are indicated in the figures by a short horizontal line. (*a*) Rocking curves for the (10 0 0) reflection. (*b*) Rocking curves for the (0 8 0) reflection. (*c*) Rocking curves for the (0 0 6) reflection. (*d*) Rocking curves for the (2 13 −3) reflection.

Table 2
The FWHM and estimated mosaicities of orthorhombic lysozyme crystals crystallized at 10 and 0 T.

The mosaic spread was estimated from FWHM with deconvolution of the instrument resolution function. The deconvoluted value is given by $\eta = (FWHM^2 - IRF'^2)^{1/2}$ (Snell *et al.*, 1997), where FWHM is the full-width at half-maximum of measured reflection rocking width and IRF' is the instrument resolution. All the FWHM values correspond to 2.36σ of the peak profile. The crystal mosaicities estimated from FWHM were in the range 0.0046–0.0075° for 10 T, averaging 0.0054° (standard deviation, 0.0009°), and ranging from 0.0054 to 0.0099° for 0 T (0.0077° average and 0.0013° standard deviation). The change in mosaicity is defined as (0 T − 10 T)/0 T. Standard deviations of FWHM obtained from seven independent observations are given in parentheses.

Reflection	FWHM (°)		Mosaic spread (°)		Difference in mosaicity (°)	Change in mosaicity (%)
	10 T	0 T	10 T	0 T		
(10 0 0)	0.0078 (0)	0.0102 (9)	0.0075	0.0099	0.0024	24.2
(0 8 0)	0.0054 (1)	0.0083 (7)	0.0049	0.0080	0.0031	38.8
(0 0 6)	0.0056 (1)	0.0079 (3)	0.0051	0.0076	0.0025	32.9
(0 4 3)	0.0051 (3)	0.0069 (1)	0.0046	0.0065	0.0019	29.2
(6 −3 −1)	0.0071 (1)	0.0085 (3)	0.0067	0.0082	0.0015	18.3
(−3 2 3)	0.0055 (0)	0.0059 (1)	0.0050	0.0054	0.0004	7.4
(−3 −2 3)	0.0056 (1)	0.0090 (1)	0.0051	0.0087	0.0036	41.4
(5 1 −2)	0.0051 (0)	0.0069 (0)	0.0046	0.0065	0.0019	29.2
(−2 13 −3)	0.0051 (5)	0.0088 (0)	0.0046	0.0085	0.0039	45.9
(2 13 −3)	0.0061 (5)	0.0088 (0)	0.0057	0.0085	0.0028	32.9
Average	0.0058	0.0081	0.0054	0.0078	0.0024	30.8

beam was approximately perpendicular to the *c* axis. The data-collection statistics are given in Table 1. The crystal grown at 10 T shows an observed maximum resolution beyond 1.13 Å, with an increased mean signal-to-noise ratio (*S/N*) and a higher fraction of intensities greater than 3σ, as shown in Table 1 and Fig. 3. The Wilson plots gave average temperature factors of 6 and 9 Å^2 for the 10 and 0 T PF data, respectively. The plots of $I/\sigma(I)$ *versus* resolution are shown in Fig. 3. It is clear that the 10 T crystals exhibit remarkably improved $I/\sigma(I)$ values compared with those of the 0 T crystals, especially at higher resolution. Significant improvements were also observed in R_{merge}, completeness, number of observed reflections and estimated mosaicity in the data processing. Furthermore, the

radiation damage was less (20%) for 10 T crystals than 0 T crystals during data collection.

3. Discussion

It is indispensable to measure rocking widths using highly collimated synchrotron radiation in order to evaluate the true effect of the enhancement of resolution maxima and the higher *S/N* ratio. Crystallization in a high magnetic field yielded longer and thicker crystals than at 0 T with higher internal quality. The larger volume of the crystal to be exposed to X-ray radiation for diffraction should bring about higher resolution maxima and *S/N* ratio, even if the internal quality of the crystal is the same. In our experiments, we observed narrower rocking widths for 10 T crystals compared with 0 T crystals using seven different crystals for both. Thus, we believe the present results are quite reliable, at least for orthorhombic lysozyme crystals. If the effect of the magnetic field has arisen from its inherent nature, we expect the improvement in crystal quality to be generalized to other proteins.

The reduction of the number of the crystals in the high magnetic field might produce larger crystal volumes. This is also considered to be favourable for high-resolution

Figure 3
Plots of average values of $I/\sigma(I)$ *versus* resolution. Comparison of diffraction intensities for 10 T (filled-in symbols and solid lines) and 0 T (open symbols and dotted lines) crystals. The plot shows the mean $I/I(\sigma)$ as a function of resolution, $1/d^2 = 4\sin^2\theta/\lambda^2$ (Å^{-2}). Standard deviations σ were obtained from merging of symmetry-related reflections (average redundancy of data was ∼4).

X-ray analysis. Furthermore, the 10 T crystals have been observed to be less damaged by X-rays. The respective average FWHM values were 0.006 and 0.008° for the 10 and 0 T crystals, *i.e.* a 30% decrease in rocking width. Thus, by a simple evaluation, a 1.4 times higher peak intensity is obtained, which agrees on average with the experimental results (Fig. 2). This fact is also shown in Fig. 3 to give extended diffraction resolution in 10 T crystals; this was also observed in diffraction patterns (data not shown).

To confirm the confidence of the differences in rocking widths with ten values in each population, we calculated a Student's *t* test and checked whether differences in the mosaicities in the 10 and 0 T populations might not be simply a consequence of undersampling. For $\nu = 9$ degrees of freedom, the result of the *t* test is significant at better than 99.99% confidence (the *P* value is less than 4.4×10^{-5}).

The orientation of the crystals (the *c* axis being parallel to the magnetic field in the present crystal) must be a consequence of the magnetic anisotropy, as quantitatively shown previously in tetragonal lysozyme crystals (Yanagiya *et al.*, 1999), although the molecular diamagnetic anisotropy that must be involved has not been determined for the present case.

We consider the inherent effects of the magnetic field that result in an enhancement of crystal quality to be as follows. The magnetic field effects were classified into three groups on the microscopic to macroscopic scale: effects on the protein solution (convection), the crystal (mosaicity) and the lysozyme molecules (molecular structure). (i) Magnetic damping of the convection produced a smaller perturbation of the concentration distribution around the crystal. (ii) The so-called mosaic blocks were better oriented along the magnetic field. (iii) Some slight changes in the three-dimensional side-chain structure of the lysozyme molecules may also have improved the crystal packing. A homogeneous magnetic field damps the natural convection even in the aqueous electrolyte solution (Sazaki *et al.*, 1999) [case (i)], as does microgravity. A magnetic field suppresses the perturbation of the concentration distribution around the growing crystals and prevents bunching of the crystal-growth steps and the incorporation of impurities (Chernov, 1984).

The magnetic anisotropy of the orthorhombic lysozyme crystal has not yet been precisely evaluated. However, it is probable that an orthorhombic crystal larger than several micrometres in size exerts an effect
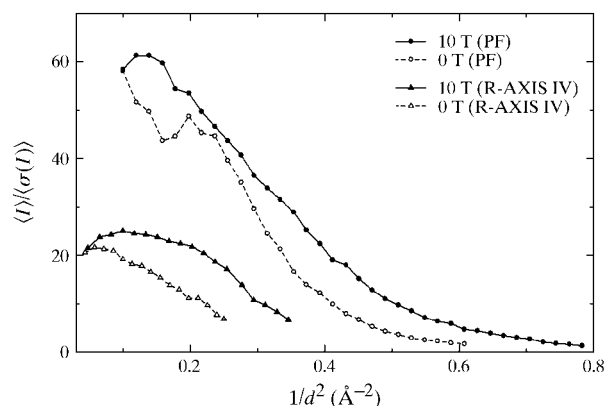
of magnetic energy one order greater than that of thermal energy [case (ii) above], as reported in the case of the tetragonal lysozyme crystal (Yanagiya *et al.*, 1999). Therefore, a magnetic field of 10 T might be able to orient mosaic blocks of several micrometres in size and improve the crystal perfection. If the improvement in the crystal perfection has been brought about by the magnetic orientation effect, an experiment annealing protein crystals at a high magnetic field should also improve the crystal perfection, resulting in higher resolution data.

A preliminary study of the refined protein structures shows that the magnetic field of 10 T has not changed the C^α-atom structure, but has caused some significant changes in the conformation of the flexible side chains of the amino-acid residues on the surface of lysozyme molecules, such as arginine [case (iii) above]. Such amino-acid residues carry electrical charge at the end of their flexible side chains and the vibrational motion of those residues might be affected by the Lorentz force. Thus, a magnetic field of 10 T might exert a significant effect on the anisotropic vibrations of those charges, possibly bringing about changes in crystal perfection. Details of the three-dimensional structure of lysozyme crystal at 10 T will be reported later.

References

Astier, J. P., Veesler, S. & Boistelle, R. (1998). *Acta Cryst.* D**54**, 703–706.

Ataka, M., Katoh, E. & Wakayama, N. I. (1997). *J. Cryst. Growth*, **173**, 592–596.

Chernov, A. A. (1984). *Modern Crystallography III*, pp. 247–256. New York: Springer–Verlag.

Colapietro, M., Cappuccio, G., Marciante, C., Pifferi, A., Spagna, R. & Helliwell, J. R. (1992). *J. Appl. Cryst.* **25**, 192–194.

Fourme, R., Ducruix, A., Riès-Kautt, M. & Capelle, B. (1999). *J. Cryst. Growth*, **196**, 535–545.

Muramatsu, Y., Ohishi, Y. & Maezawa, H. (1988). KEK Internal Report, pp. 87–10.

Otwinowski, Z. & Minor, W. (1997). *Methods Enzymol.* **276**, 307–326.

Press, W. H., Flannery, B. P., Teukolsky, S. A. & Vetterling, W. T. (1995). *Numerical Recipes in C: The Art of Scientific Computing*, pp. 681–688. Cambridge University Press.

Rossman, M. G. & van Beek, C. G. (1999). *Acta Cryst.* D**55**, 1631–1640.

Rothgeb, T. M. & Oldfield, E. (1981). *J. Biol. Chem.* **256**, 1432–1446.

Sakurazawa, S., Kubota, T. & Ataka, M. (1999). *J. Cryst. Growth*, **196**, 325–331.

Sasaki, S. (1989). *Rev. Sci. Instrum.* **7**, 2417–2420.

Sato, T., Sazaki, G., Katsuya, Y. & Matsuura, Y. (1999). *Abstracts of the XVIIIth International Union of Crystallography Congress and General Assembly, Glasgow.*

Sazaki, G., Durbin, S. D., Miyashita, S., Ujihara, T., Nakajima, K. & Motokawa, M. (1999). *Jpn J. Appl. Phys.* **38**, 842–844.

Sazaki, G., Yoshida, E., Komatsu, H., Nakada, T., Miyashita, S. & Watanabe, K. (1997). *J. Cryst. Growth*, **173**, 231–234.

Snell, E. H., Cassetta, A., Helliwell, J. R., Boggon, T. J., Chayen, N. E., Weckert, E., Hölzer, K., Schroer, K., Gordon, E. J. & Zagalsky, P. F. (1997). *Acta Cryst.* D**53**, 231–239.

Snell, E. H., Weisgerber, S., Helliwell, J. R., Weckert, E., Hölzer, K. & Schroer, K. (1995). *Acta Cryst.* D**51**, 1099–1102.

Wakayama, N. I. (1998). *J. Cryst. Growth*, **191**, 199–205.

Wakayama, N. I., Ataka, M. & Abe, H. (1997). *J. Cryst. Growth*, **178**, 653–656.

Yanagiya, S., Sazaki, G., Durbin, S. D., Miyashita, S., Nakajima, K., Komatsu, H., Watanabe, K. & Motokawa, M. (1999). *J. Cryst. Growth*, **196**, 319–324.

Yanagiya, S., Sazaki, G., Durbin, S. D., Miyashita, S., Nakajima, K., Komatsu, H., Watanabe, K. & Motokawa, M. (2000). *J. Cryst. Growth*, **208**, 645–650.